Published in final edited form as:
Methods. 2010 January ; 50(1): 20. doi:10.1016/j.ymeth.2009.05.016.

In vivo microCT imaging of liver lesions in small animal models

Lucia Martiniova[1,3], **Daniel Schimel**[2], **Edwin W. Lai**[1], **Andrea Limpuangthip**[1], **Richard Kvetnansky**[3], and **Karel Pacak**[1]

[1]Section on Medical Neuroendocrinology, Eunice Kennedy Shriver National Institute of Child Health and Human Development, National Institutes of Health, Bethesda, Maryland 20892-1109, USA.

[2]National Institute of Neurological Disorders and Stroke/ Mouse Imaging Facility, Charles River Labs, Bethesda, MD, 20892, USA

[3]Institute of Experimental Endocrinology, Slovak Academy of Sciences, Bratislava, Slovakia, 83306

Abstract

Three-dimensional micro-computed tomography (microCT) offers the opportunity to capture images liver structures and lesions in mice with a high spatial resolution. Non-invasive microCT allows for accurate calculation of vessel tortuosity and density, as well as liver lesion volume and distribution. Longitudinal monitoring of liver lesions is also possible. However, distinguishing liver lesions from variations within a normal liver is impossible by microCT without the use of liver- or tumor-specific contrast-enhancing agents. The combination of microCT for morphologic imaging with functional imaging, such as positron emission tomography (PET) or single photon emission tomography (SPECT), offers the opportunity for better abdominal imaging and assessment of structure discrepancies visible by functional imaging.

This manuscript describes methods of current microCT imaging options for imaging of liver lesions compared to other imaging techniques in small animals.

Keywords

pheochromocytoma; anatomical imaging; microCT; liver lesions

1. Introduction

Using animal models is important for accelerating the introduction of experimental drugs into clinical research. Small mammals provide the possibility for thorough and rapid monitoring of both implanted and spontaneous lesion development, growth, and response to various therapeutic options. Many murine models have been developed to study tumorigenesis. Two examples of such engineered murine models are MMTV-HER-2/*neu* [1] or WAP-*p53* [2]. In these models, formation of mammary tumors occur along with pulmonary and lymph node metastases. Orthotropic transplantation of human tumors into immunodeficient mice induces widespread metastases into the liver, bone, and the lungs [3,4]. Other options for metastatic

Mailing address for corresponding author: Karel Pacak, MD, PhD, DSc, Professor of Medicine, NICHD, NIH, Building 10 Room 1E-3140, 10 Center Drive MSC-1109, Bethesda, Maryland, 20892-1109 USA, karel@mail.nih.gov, Phone: 301-402-4594, Fax number: 301-402-4712.

developments are intravenous (*i.v.*) or intracardiac cancer cell injections into immunodeficient mice, which induce lung or bone metastases [5].

Conventional cancer treatment usually fails because of the lost control over metastases resulting in metabolic collapse and organ failure. Consequently, it is important to study experimental drug options, especially initially, using metastatic animal models. In this manuscript, we present our experience and observations with an animal model of metastatic pheochromocytoma using micro computed tomography (microCT). With this model, animals rapidly develop liver lesions. Thus, they are very suitable for studying potential experimental therapies, since the prognosis of patients with metastatic lesions to vital organs such as the liver and the lungs is worst [6]. We have also reported development of other organ metastases found in the lungs, bone, adrenal gland, and ovaries [7]. While the aggressive metastatic model can be used for preclinical experimental therapies, the key element is to monitor metastatic lesions longitudinally and non-invasively in animals. Furthermore, this manuscript discusses anatomical imaging microCT for the evaluation of liver lesions and also introduces the use of magnetic resonance imaging (MRI) and positron emission tomography (PET) techniques.

2. Description of methods

2.1. Anatomical imaging - microCT

In recent years, developments in biomedical research has focused on the development of microCTs with the application for studying bone and lung disease, for which the natural and significantly visible contrast between bone, air and the surrounding soft tissues is met [8]. The main purpose for development of small-animal X-ray CTs is for use in imaging and monitoring the progression of various diseases over time (longitudinal imaging), tumor development and growth, visualization of blood vessels and angiogenesis, and following the tumors and various disease responses to preclinical therapeutic intervention [9,10]. This is all possible due to its excellent spatial resolution and the possibility of acquiring detailed anatomical structures. However, the lack of intra-abdominal structural contrast in CTs often jeopardizes the detection of abdominal tumors.

2.2. MicroCT systems

The principle of microCT is the use of the attenuation of X-rays by various tissues spaced within angular intervals. This collection of signals is processed by applying the reconstruction algorithms, usually a back-projection algorithm, which allows creating a 3-dimential volumetric data set consisting of representative pixels. Each pixel in the image has a value that can be mapped to the density of the tissue being imaged. This scale is referred to as the CT number or the Hounsfield unit (HU), which is based on water being zero. Tissues that are less dense than water are negative on the scale and the higher density materials, are positive [11]. HU can be used for quantification and for distinguishing tissue structures, especially after the use of contrast agents.

For longitudinal studies it is very important to achieve the most efficient and least toxic method of effective visualization of disease progression in small animals. This involves decreasing the radiation dose from microCT acquisition and involving the use of specific contrast agents. One of the most important issues is the actual handling of the animals and temperature conditions during scanning and recovery. Animals suffer from rapid heat loss while they are under the anesthesia. Maintaining the heating of animals during the scanning procedure is beneficial not only to their recovery time, but also for regulating the breathing processes which effects both scanning time and image quality.

The images presented in this manuscript were acquired on the microCAT II (Siemens Preclinical Solutions, Knoxville, TN). It is a high resolution CT system designed specifically for imaging small animals such as mice and rats. This system consists of a low-energy x-ray tube (x-ray energy, 30–55 kVp), a high-resolution phosphor screen, a charge-coupled-device detector, and a precision-motion translation stage. The detector and x-ray source rotate around a fixed bed, allowing the mouse to remain in the same horizontal position in the CT scanner. The images were acquired at 55 kVp with an anode current of 500 μ*A* and a shutter speed of 500 milliseconds. Scans were completed over 360 degrees of rotation of the X-ray tube with 450 projections to increase signal-to-noise (SNR). Reconstructions were performed using a cone-beam filtered back projection algorithm. The axial field of view (FOV) was set to 4.6 cm with an inplane spatial resolution of 91 μm and slice thickness of 91 μm as well. The reconstruction image size was 910 × 910 pixels, and the number of slices depended on the chosen field of view in all dimensions. Final reconstructed data were analyzed using commercially available visualization software (Amira, Version 3.1, TGS, San Diego, CA). The radiation dose for each microCT scan also varies with the chosen size of FOV. In our system, FOV 4.6 cm and a spatial resolution of 91 μm the radiation dose was 7 REM (70mSv). This radiation dose was measured by Radiation Alert® PEN dosimeter. The PENS are rugged direct-reading carbon fiber dosimeters that measure and directly display the radiation dose or quantity of gamma and x-ray exposure. Though this is object to measure personal accumulated dose or quantity of gamma and X-ray radiation, it still can be used for easy and quick dose measurements for different parametric set-up inside of the FOV. After securing the acquisitions, the dose amount is easy to read, by holding the dosimeter up to a light source to view the scale inside this dosimeter. The fiber inside moves across a predetermined scale, thus displaying the level of radiation exposure. This provides immediate and accurate results without external laboratory analysis. The total scan time for each microCT scan was approximately 10–20 minutes, with variations due to respiratory rate.

Other examples of microCT imaging systems are manufactured by General Electric Medical Systems (model RS-9, London, Ontario) (12), volumetric CT scanner (NFR-Polaris-G90; NanoFocusRay, Iksan, Korea) [12] used for detection of liver metastases and flat-panel volumetric computed tomography (fpVCT) [13].

2.3. Respiratory gated microCT acquisitions

To improve the image quality, respiratory triggering is used to reduce movement artifacts from animal breathing and internal organ movement and images were captured after the peak of expiration and beginning of the peak of inspiration, when the period without movement was longest and usually matching with the 500 milliseconds shutter speed. The study by Cavanaugh et al. [14] focuses on the effect of animal preparation and quality of respiratory-gated microCT imaging. There are several factors affecting the respiration of animals. For example, it is known that mice that have been anesthetized with higher doses of isoflurane develop breathing with a particular respiration pattern characterized by gasping breaths separated by long intervals [14]. In this case, it is appropriate to monitor the respiration with a respiration pillow that will transfer the information about movement from respiration into the imaging acquisition system, allowing the machine to acquire images only when the breathing is in a period or expiration or inspiration. Another option to control breathing would be mouse ventilation, a technique used mostly for the visualization of lung parenchyma because of improved lung contrast [14]. Recently, we have presented [7] that small liver lesions (0.5 mm in diameter) would not be possible to visualize without respiratory-gating, and small vessels could be mistakenly considered as liver lesions.

2.4. Anesthesia for microCT

There are many anesthesia options for animals. Widely used are intramuscular and intraperitoneal injections of combinations of Ketamine and Diazepam [11] or Ketamine and Xylazine, and isoflurane inhalation [15]. Ketamine hydrochloride is a cyclohexylamine analogue, which produces, in primates, a state of unconsciousness and somatic analgesia but no muscular relaxation. Ketamine tends to stimulate cardiopulmonary function and often enhances muscle tone to the extent that tremors or even tonic-clonic convulsions are produced. Xylazine hydrochloride is a potent hypnotic with powerful central muscular relaxant properties. Its main disadvantage is that it interfering with normal electrical activity in the heart producing significant cardiac arrhythmias in all species, especially following intravenous administration [15]. However, a combination of Ketamine and Xylazine can be useful, allowing animals to be in deep sleep even for surgical procedures.

Regarding our studies, we chose to inject a cocktail of Ketamine (100 mg/ml)/Xylazine (20 mg/ml) solution in 3:1 ratio. For our pheochromocytoma model we chose an intramuscular injection of 0.1 ml of Katamine/Xylazine which allowed animals to sleep for 30 minutes. Constant monitoring of cardiac and respiratory activity was preformed while animals were under anesthesia. The release of catecholamines from tumor cells coupled with Ketamine injections, have the potential to produce severe tachycardia in mice and in mice with numerous liver pheochromocytomas, death has been observed with Ketamine/Xylazine anesthesia. Ketamine/Xylazine is catabolyzed by the liver [16] and in mice with severe liver tumor burden injections of which can lead to hepatocyte damage and death (personal observation). We currently recommend Ketamine/Xylazine not be used in mice with severe liver tumor burden for fear of premature death.

Isoflurane inhalation is a practical alternative to Ketamine/Xylazine injections because it allows for longer acquisition times, minimal animal handling, ease of anesthetic control, and quick animal recovery times. The primary disadvantages are the initial cost of equipment and the need to control human gas exposure. Though Isoflurane has little direct affect on the heart, it does cause peripheral vasodilation of the blood vessels, which results in decreased blood pressure. After careful consideration of experiences with anesthesia in the metastatic pheochromocytoma model, we used Isoflurane/O_2 (1.5–5% v/v) for all microCT imaging. A respiratory pillow was placed on the chest or back of the mouse to record the respiratory rate of the mouse while under anesthesia. Appropriate care was taken to maintain body temperature at 37°C during the scanning period and recovery from anesthesia after scanning.

2.5. Contrast agent for microCT

The detection of soft tissue lesions is possible if a special contrast agent is used. In humans, water-soluble contrast agents are frequently used; however, this does not apply well to small animals. One reason is that the microCT technology is not as rapid in capturing images as it is in humans, with acquisition times between 10–20 minutes in animals versus seconds in humans [15]. Thus, the water-soluble contrast agents used in human studies, are rapidly cleared by human kidneys within minutes, are in cleared within seconds in small animals, allowing insufficient time to acquire microCT images. Another possibility for adaptation of contrast agents used in humans would be with iodine origin. These compounds are the most extensively used CT contrast agents and distribute into the whole liver tissue evenly within a few minutes of bolus injection. Thus, the result is a limited contrast effect of the blood flow inside the arteries or veins and the interested tissue areas which also diminish quickly [16]. For these reasons, it is desirable to develop contrast agents that distribute to liver tissues with a retention time sufficient enough to acquire CT image and provide for adequate contrast enhancement.

There might be possibilities to study human contrast agents, for example with the help of volumetric computed tomography (VCT). This new technology combines the advantages of both microCT and clinical CT scanners. Instead of multiple detector rows [19,20], as in clinical scanners, two flat-panel detectors are used, which have pixel sizes of <0.04 mm2 and offer excellent imaging performance, thus reducing acquisition times to a matter of seconds [21]. Another example is an ultra-fast volume computed tomography-angiography (vCTA) which is feasible for studying of various contrast agents in mice [22].

MicroCT scanners are becoming more readily available at the research centers and, from the aforementioned options; there are also many new technologies to choose from. Nevertheless, handling of animals is also very important and administration of various contrast agents needs to be performed carefully (usually done by tail vein injection). Nude mice are easiest to work with since there is great visibility of tail veins after heating of animals. Though the quickest way is to use heating lamp, the nude mice can easily become overheated. Using a water circulating heating pad is also very effective for this purpose. We use 30 G needle while an animal is under anesthesia or placed in plastic restrainer.

2.6. Liver specific contrast agent: detection of liver metastasis in an experimental model of animal pheochromocytoma

Recently we have established an animal model of metastatic pheochromocytoma [17]. Metastatic liver lesions developed as early as three weeks after mouse pheochromocytoma (MPC) cells are intravenously injected, the tumors and vessels appearing as negative on the contrast enhanced background of the liver. This was achieved by injection of liver specific Fenestra™ Liver Contrast (Fenestra™ LC; Advanced Research Technologies, Inc). The tail veins of the mice were cannulated, and approximately 0.3 ml of the contrast agent Fenestra™ LC was injected (0.013 ml of Fenestra™ LC /gram of body weight of animal) [18–20]. The Fenestra™ LC has been introduced and described in detail previously [21,22]. Briefly, this contrast agent is composed of chylomicron-remnant-like particles that consist of a lipophilic core that contains the opacifying agent 2-oleoylglycerol 1,3-bis[7-(3-amino-2,4,6-triiodophenyl) heptanoate] [15]. Once secreted by the liver, the triglyceride core is metabolized and excreted through the biliary system [19]. This lipophilic contrast agent clears slowly from the vascular pool and accumulates in the liver parenchyma. In Fig. 1 and Fig. 2 we present the example of an animal model of metastatic pheochromocytoma with liver lesion development. Female athymic nude mice (NCr-nu, Taconic, Germantown, NY) were injected by tail vein with $1–5\times10^6$ mouse pheochromocytoma (MPC) cells. MPC cells were grown in tissue culture flasks, without collagen, in DMEM medium described in detail [17].

All animal experiments with microCT imaging followed the same dosing protocol. Based on our experience, 3 h after *i.v.* injection of Fenestra™ LC, the highest uptake of Fenestra™ LC in liver was observed, and the highest SNR between liver and liver lesions was achieved. In the study of Suckow et al. [23], a stable level of liver contrast was reached after 90 min and remained constant up to 4 h post-injection mice.

The detection of liver lesions is impossible without the use of contrast-enhancing agents though, even then, the problem of distinguishing small vessels and small liver tumors is an issue. Therefore, we have established dual-phase contrast enhancement [7], in which two different scan acquisitions are performed. First, we acquired a scan immediately after intravenous injection of the contrast agent, allowing the visualization of vessels in liver. Then, a second scan was performed three hours after uptake of the contrast agent. At that point, the contrast enhanced liver parenchyma, vessels, and tumors were all distinguished. Comparing the first scan, in which vessels still contained contrast agent and appeared the same as liver tissue, to the second scan, we can recognize whether the questionable area is a small vessel or a small tumor. Fig. 1 represents transverse, coronal and sagittal microCT views acquired three

hours post contrast injection (Fenestra^{TM} LC). Liver lesions developed from 1–3mm in diameter. The arrow points to the same lesions in all views. After reconstruction of raw data, HU (Fig. 1D) helped create the 3D surface-rendered images of mice with liver lesions (Fig. 2A, B). The lobes of liver (blue) are well defined, as are the vasculature within. Due to the different contrast enhancement and HU, we were able to separate liver tumors (green) from vessels (red). All figures were created in Amira, (Version 3.1, TGS, San Diego, CA). The sensitivity of HU can be great tool for measuring precisely dimensions and volumes of individual tumors and thus better evaluate tumor growths rates. Tumor volumes are often better for estimating treatment responses compared to plane diameters measurements.

2.7. Vascular contrast agent and other contrast agents

Angiogenesis is a key element of a developing cancer by providing the new blood supply to a tumor and subsequently allowing for its malignant progression [24]. However, imaging the angiogenic circulation in small animals is extremely challenging because the vessels are small and beyond the resolution limits of clinical systems [25]. Contrast agents need to stay in the blood stream long enough to acquire microCT images, and this represents a great advantage for performing fine morphological imaging.

Weichert et al. [19] have developed a new class of iodinated blood-pool emulsions that demonstrate adequate kinetic properties in rabbits and rats; for example, the iodinated lipid emulsion blood-pool contrast agent Fenestra^{TM}Vascular Contrast, (Fenestra^{TM}VC), Alerion Biomedical, San Diego, CA, USA (50 mg I/ml). In the blood-pool variant, the polyiodinated triglyceride emulsion contains polyethylene glycol-modified phospholipids (ITG-PEG), which delay liver sequestration of the particle from the blood [26]. The time course of this procedure has been described by Ford et al. [27], after injection of a 0.01 mL/g body weight dose into C57BL/6 mice. Along with the use of the iodinated blood-pool agent, major organs were visualized including major vessels, the liver parenchyma from vasculature, the spleen, and the gastrointestinal tract. The same was reported as a contrast agent for vascular imaging of tumors in small animals [25]. In these experiments, the blood pool contrast agent containing iodine was used with a concentration of 130 mg/mL Fenestra^{TM}VC. Although, they did not apply this contrast agent to visualize liver lesions, they did successfully detected tumors implanted in the neck region and visualize their vascular architecture in rats. Furthermore, they were also able to distinguish tumor's mass and the central portion being poorly vascularized, since the contrast agent targets the blood-pool and is able to resolve very thin vessels in the tumor. For visualization of liver tumors in nude mice and their structures, (Fenestra^{TM}VC) might not be able to distinguish between a vascular tumor and vascularity of the liver, depending of the lesion size and surrounding vasculature.

From other possible contrast agents, liposomal iodine formulations have been offered to be a promising contrast agent for liver CT imaging. Wei et al. described a new liposomal iodine formulation based on multivesicular liposome structures. Multivesicular liposome (MVL) usually contains a larger internal space, which allows for more drug loading [16]. They were shown to distribute evenly in the hepatic sinusoid between hepatic plates and the endothelium after intravenous injection and were still detected in liver 40 min after injection. A significant and persistent enhancement to CT value in the liver was observed in CT imaging studies. Compared to the conventional extracellular iodine agent Iohexol, the MVL formulation is easier to administer and requires much lower doses, while providing greater and longer lasting liver imaging enhancement. Therefore, we perceive it to have great potential as a new and superior contrast enhancement agent for CT imaging of the liver [16].

2.8. MicroCT and co-registration with other imaging techniques used for localization of liver lesions

Combining the anatomical (CT and/or MRI) and functional (PET, single photon emission tomography (SPECT)) imaging can currently give the most thorough information about study subjects. Currently, all mentioned modalities could be combined in the same machine. The CT components are important for anatomical support and can be used also for improving the reconstruction process. Until now, not many investigators use all of the advantages of mentioned combinations. The use of tissue/tumor contrast agents would create the proper localization information, but also could be used for quantification purposes and image reconstruction improvements. Most of the PET tracers are highly sensitive for their molecular targets, but provide relatively little anatomical information. A great example of multimodal imaging and localization of metastatic lesions is described in [28], where metastatic lung lesions are successfully visualized and all challenges of combined imaging techniques and data reconstructions are effectively managed.

However, co-registration of anatomical and functional images can be very challenging, particularly if the images are acquired on separate machines. This involves changing the positioning of the animal in time, which is especially important for monitoring liver lesions. It is possible to use fiducial markers for both techniques and rotate animal reconstructed data accordingly; yet, it still would be very difficult to recognize small liver lesions. The other challenge would be reconstructing data at the same format and use fusion software where all rotation and positioning would be possible. From our experience we recommend the AMIDE software [29]. Fig. 3 represents the microCT /PET fusion of liver lesions in pheochromocytoma mouse model with Amide software. The software is free and includes features like arbitrary orientation, thickness, and time period slice viewing of a data set. Multiple data sets can be loaded and viewed at once, with either linked or fused views. Each data set can be viewed from any orientation. Fusing can be done by blending or overlay. Imports raw data files (8 bit, 16 bit, 32 bit, float, etc). It imports Acr/Nema 2.0, Analyze (SPM), DICOM 3.0, InterFile 3.3, ECAT 6/7, and Gif87a/89a (using the (X)medcon/libmdc). It imports most clinical DICOM files. InterFiles can be created also in free software ImageJ (Plugins/NucMed/Save as InterFile) and be back imported into AMIDE. Another option would be using free available software MIPAV. This software also can open all raw data files mentioned above, and has many great features, including image fusion, volume measurements of liver lesions [7].

2.9. Applications of microCT in drug discovery and future perspectives in microCT imaging designs

Responses to various therapeutic drugs can be evaluated by their decreased tumor size by anatomical imaging and by their physiological changes by functional PET-imaging. However, the PET/CT machines would address both issues at the same time.

The future prospective for microCT imaging is creating machines with the same competence as clinical CTs are in their speed and efficiency in acquiring images. This would help with the correlation of structural anatomy from CT (including the attenuation correction and transmission maps great for calibration curves) with physiological information acquired from PET or SPECT where the limitation is structural size dependence.

3. Conclusion

MicroCT technology appears to be a promising and useful tool for visualization of the anatomy of small animals with excellent spatial resolution. This technology is also widely used by numerous investigators and is becoming very popular for imaging of high-contrast structures, such as bones. With the use of specific contrast agents, MicroCT could also be used for

monitoring tumor growth in liver. Recently, it has become possible to monitor changes in the 3D architecture of organs, tumors, and its microvasculature which may have an immediate impact on the global understanding in the evaluation of experimental therapies. Development of multimodality systems that combine anatomical and functional imaging should expand the applications of microCT, and, specifically, improve visualization and characterization of tumors in animal models.

Acknowledgments

We would like to thank the contributions and assistance of Dr. Arthur S. Tischler for his help and guidance. We thank Dr. Brenda Klaunberg and the intramural shared resources for microCT imaging in the Mouse Imaging Facility. We thank Eli Thompson for his assistance with the animals and Mrs. Evin O'Keeffe for her help with editing. This research was supported (in part) by the Intramural Research Program of the NIH\NICHD and APVV-0148-06 (to R.K.). The authors have no conflict of interest to disclose.

References

1. Guy CT, Webster MA, Schaller M, Parsons TJ, Cardiff RD, Muller WJ. Proc Natl Acad Sci U S A 1992;89:10578–10582. [PubMed: 1359541]
2. Lin SC, Lee KF, Nikitin AY, Hilsenbeck SG, Cardiff RD, Li A, Kang KW, Frank SA, Lee WH, Lee EY. Cancer Res 2004;64:3525–3532. [PubMed: 15150107]
3. An Z, Jiang P, Wang X, Moossa AR, Hoffman RM. Clin Exp Metastasis 1999;17:265–270. [PubMed: 10432012]
4. Hoffman RM. Invest New Drugs 1999;17:343–359. [PubMed: 10759402]
5. Minn AJ, Gupta GP, Siegel PM, Bos PD, Shu W, Giri DD, Viale A, Olshen AB, Gerald WL, Massague J. Nature 2005;436:518–524. [PubMed: 16049480]
6. Mizuno O. Nippon Naibunpi Gakkai Zasshi 1994;70:1039–1046. [PubMed: 7851622]
7. Martiniova L, Kotys MS, Thomasson D, Schimel D, Lai EW, Bernardo M, Merino MJ, Powers JF, Ruzicka J, Kvetnansky R, Choyke PL, Pacak K. J Magn Reson Imaging 2009;29:685–691. [PubMed: 19243052]
8. Paulus MJ, Gleason SS, Kennel SJ, Hunsicker PR, Johnson DK. Neoplasia 2000;2:62–70. [PubMed: 10933069]
9. Marx J. Science 2003;302:1880–1882. [PubMed: 14671264]
10. Maehara N. Eur Radiol 2003;13:1559–1565. [PubMed: 12835967]
11. Johnson KA. Toxicol Pathol 2007;35:59–64. [PubMed: 17325973]
12. Kim HW, Cai QY, Jun HY, Chon KS, Park SH, Byun SJ, Lee MS, Oh JM, Kim HS, Yoon KH. Acad Radiol 2008;15:1282–1290. [PubMed: 18790400]
13. Wessels JT, Busse AC, Mahrt J, Dullin C, Grabbe E, Mueller GA. Cytometry A 2007;71:542–549. [PubMed: 17598185]
14. Cavanaugh D, Johnson E, Price RE, Kurie J, Travis EL, Cody DD. Mol Imaging 2004;3:55–62. [PubMed: 15142412]
15. Weber SM, Peterson KA, Durkee B, Qi C, Longino M, Warner T, Lee FT Jr, Weichert JP. J Surg Res 2004;119:41–45. [PubMed: 15126080]
16. Wei X, Geng F, He D, Qiu J, Xu Y. Conf Proc IEEE Eng Med Biol Soc 2005;6:5702–5705. [PubMed: 17281551]
17. Martiniova L, Lai EW, Elkahloun AG, Abu-Asab M, Wickremasinghe A, Solis DC, Perera SM, Huynh TT, Lubensky IA, Tischler AS, Kvetnansky R, Alesci S, Morris JC, Pacak K. Clin Exp Metastasis 2009;26:239–250. [PubMed: 19169894]
18. Bakan DA, Lee FT Jr, Weichert JP, Longino MA, Counsell RE. Acad Radiol 2002;1(9 Suppl):S194–S199. [PubMed: 12019866]
19. Weichert JP, Lee FT Jr, Chosy SG, Longino MA, Kuhlman JE, Heisey DM, Leverson GE. Radiology 2000;216:865–871. [PubMed: 10966724]
20. Lee FT Jr, Chosy SG, Naidu SG, Goldfarb S, Weichert JP, Bakan DA, Kuhlman JE, Tambeaux RH, Sproat IA. Radiology 1997;203:465–470. [PubMed: 9114106]

21. Weichert JP, Longino MA, Bakan DA, Spigarelli MG, Chou TS, Schwendner SW, Counsell RE. J Med Chem 1995;38:636–646. [PubMed: 7861412]
22. Bakan DA, Longino MA, Weichert JP, Counsell RE. J Pharm Sci 1996;85:908–914. [PubMed: 8877877]
23. Suckow CE, Stout DB. Mol Imaging Biol 2008;10:114–120. [PubMed: 18204990]
24. Folkman J. Eur J Cancer 1996;32A:2534–2539. [PubMed: 9059344]
25. Badea CT, Hedlund LW, De Lin M, Boslego Mackel JF, Johnson GA. Contrast Media Mol Imaging 2006;1:153–164. [PubMed: 17193692]
26. Bakan DA, Doerr-Stevens JK, Weichert JP, Longino MA, Lee FT Jr, Counsell RE. Am J Ther 2001;8:359–365. [PubMed: 11550077]
27. Ford NL, Graham KC, Groom AC, Macdonald IC, Chambers AF, Holdsworth DW. Invest Radiol 2006;41:384–390. [PubMed: 16523021]
28. Deroose CM, De A, Loening AM, Chow PL, Ray P, Chatziioannou AF, Gambhir SS. J Nucl Med 2007;48:295–303. [PubMed: 17268028]
29. Loening AM, Gambhir SS. Mol Imaging 2003;2:131–137. [PubMed: 14649056]

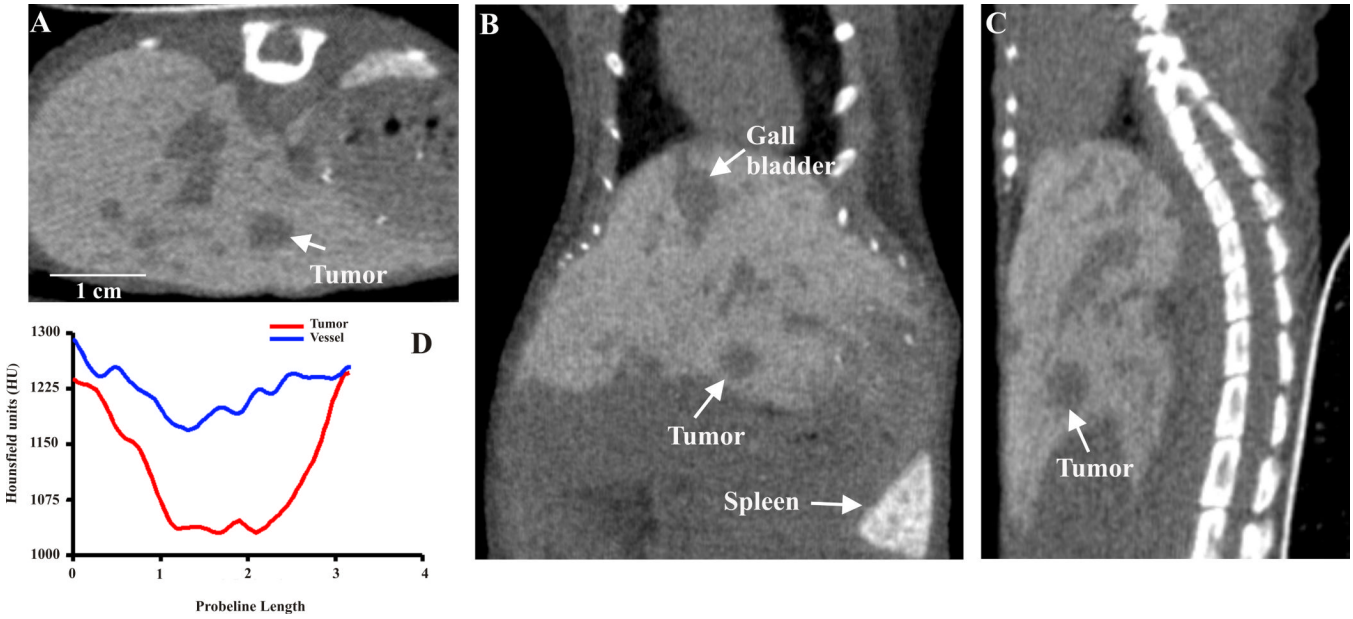

Fig. 1.

Micro computed tomography (CT) images acquired after hepatocyte-specific contrast (Fenestra™ LC) 3 hours post injection. Transverse (A), coronal (B), and sagittal (C) views of the abdomen in a nude mouse with developed liver lesions. The arrow points to the same lesions in all views. Line-profile data (D) visualizing the liver parenchyma (1220–1240 HU) – trough liver tumor (1025–1060 HU) in contrast to the vasculature (1170–1300 HU).

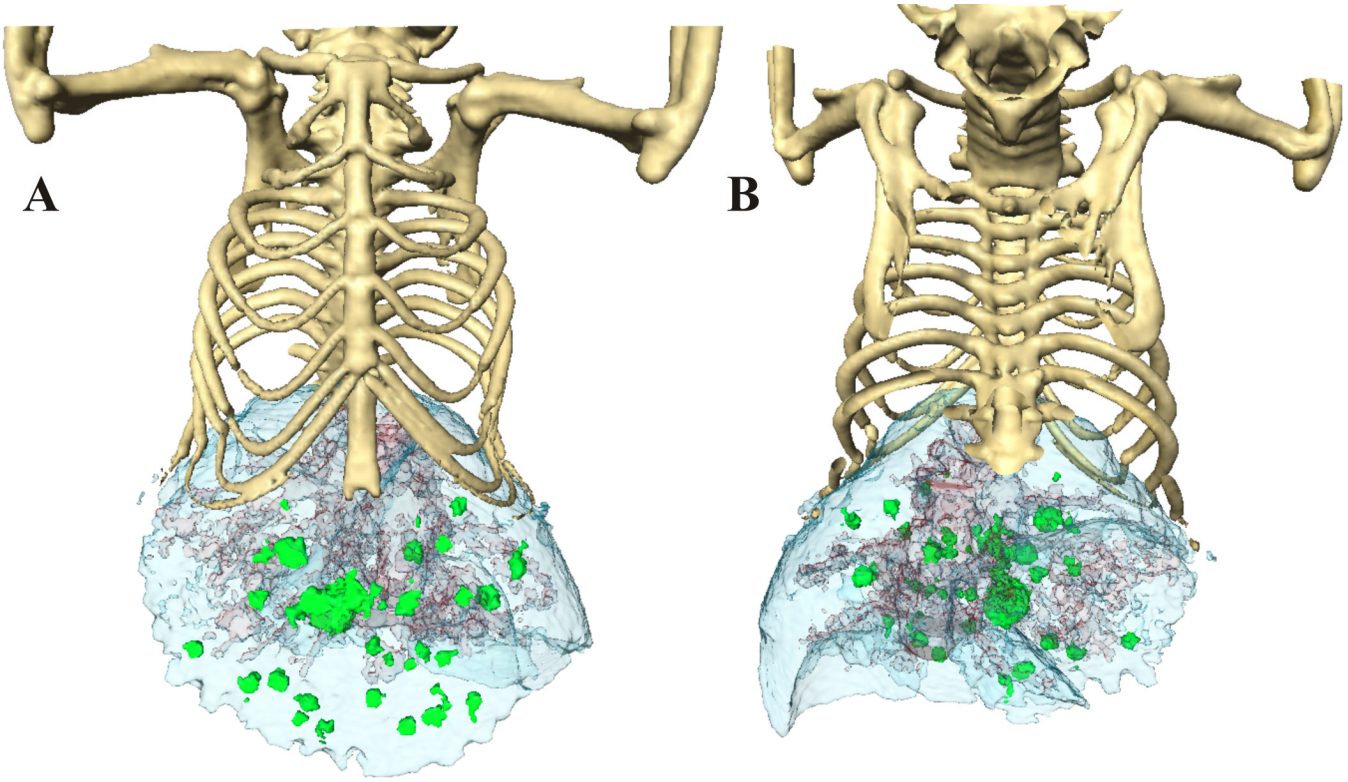

Fig. 2.

The anterior (A) and posterior image (B) surface-rendered images of mouse with liver lesions after 3 hours of contrast enhancement. The lobes of liver (blue) are well defined, as well as the vasculature in it. Due to the different contrast enhancement and HU, we were able to separate the liver tumors (green) from the liver vessels (red).

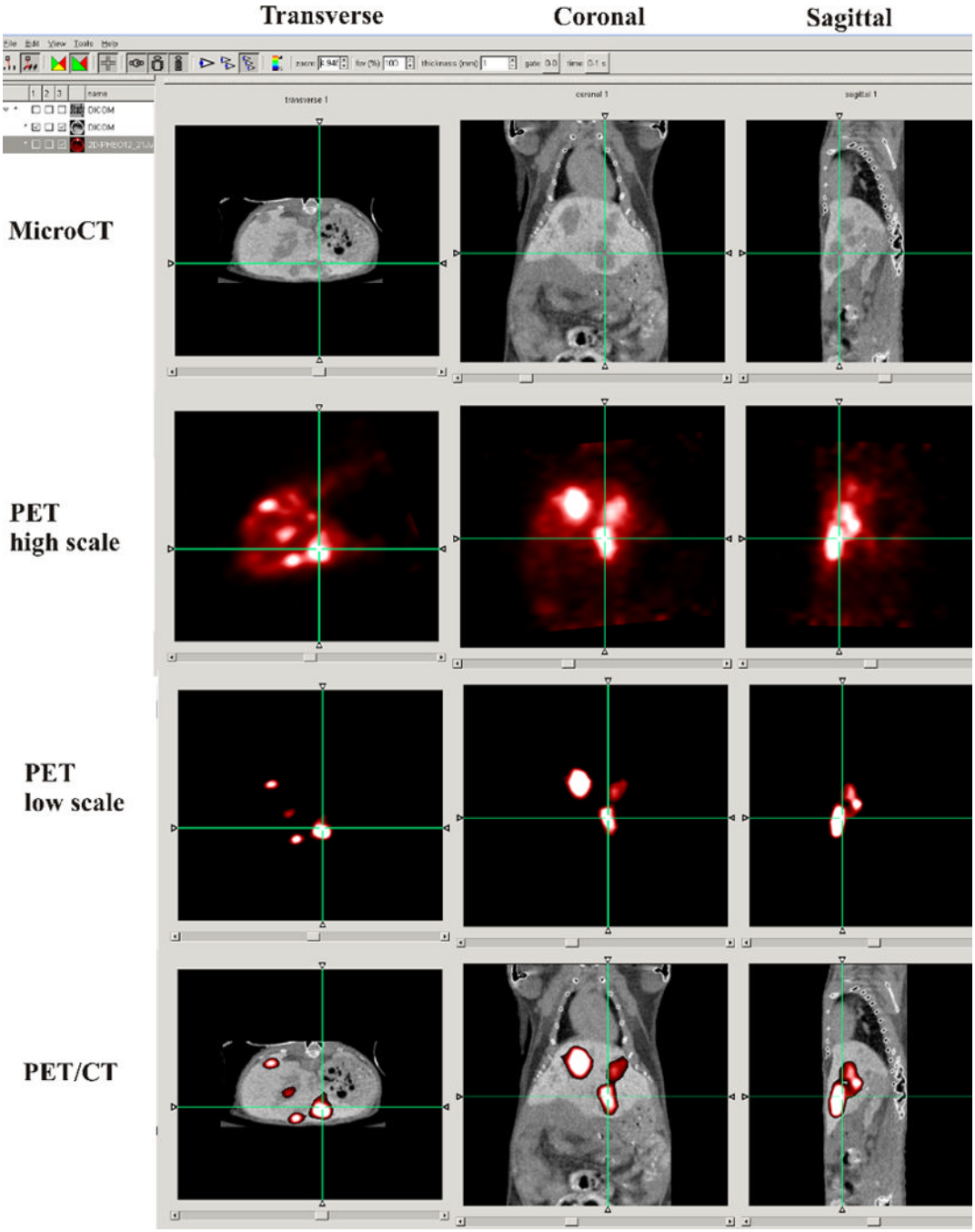

Fig. 3.

MicroCT/PET fusion was performed in AMIDE software. MicroCT scan with the liver contras agent was performed as descried in section 2.6. PET acquisition were performed on Advanced Technology Laboratory Animal Scanner (ATLAS) scanner 60 min after administering 3.5–3.9 MBq of [^{18}F]-6F–Dopamine. The PET image is presented with two different brightness scale as low and high for better visualization of the all body of the animal with [^{18}F]-6F–Dopamine PET. The microPET scan was performed on ATLAS scanner 1 day after the microCT. The crosshairs linking of the axial, coronal, and sagittal reformatted images, visualize of the same liver lesion on microCT and PET.